IOP Conference Series: Earth and Environmental Science

PAPER • **OPEN ACCESS**

Research and calculation of the levels of higher harmonics of rotary electric machines in active-adaptive networks

To cite this article: I V Khomenko *et al* 2023 *IOP Conf. Ser.: Earth Environ. Sci.* **1254** 012040

IOP Conf. Series: Earth and Environmental Science 1254 (2023) 012040 doi:10.1088/1755-1315/1254/1/012040

Research and calculation of the levels of higher harmonics of rotary electric machines in active-adaptive networks

I V Khomenko[1], V P Nerubatskyi[2], O A Plakhtii[2], D A Hordiienko[2] and D A Shelest[2]

[1] National Technical University "Kharkiv Polytechnic Institute", 2 Kyrpychova Str., Kharkiv, 61002, Ukraine

[2] Ukrainian State University of Railway Transport, 7 Feierbakh Sq., Kharkiv, 61050, Ukraine

E-mail: igor.v.khomenko@gmail.com, NVP9@i.ua, a.plakhtiy1989@gmail.com, D.Hordiienko@i.ua, D.Shelest@gmail.com

Abstract. In the materials of the article, the parameters of the higher harmonics of the groove frequency are analyzed, which affect the reliability of the operation of electrical equipment and the loss of electrical energy in active-adaptive networks. The influence of higher harmonics of rotary electric machines on the modes of operation of active-adaptive networks and their power equipment is considered. It was established that this influence depends on the energy level of higher harmonics and the modes of operation of active-adaptive networks. A technique is proposed that allows determining the levels of groove harmonic components in the phase windings of electric machines. The calculation of the energy level of higher harmonics was carried out taking into account the electromagnetic asymmetry of rotating electric machines and asymmetric modes of operation of three-phase electric networks using the method of phase coordinates. The obtained results are based on theoretical and experimental studies of the influence of higher harmonics of rotating electric machines on the modes of operation of electrical networks and power energy equipment.

1. Introduction

The quality of electrical energy significantly affects the reliability and efficiency of electrical networks and power equipment. One of the important indicators of the quality of electrical energy is the level of higher harmonics, which causes non-sinusoidal modes of operation of electrical networks [1, 2].

The nature of higher harmonics is diverse. The influence of higher harmonics of rotating electric machines (synchronous generator, asynchronous motor, etc.) on the operating modes of the electric network has not been sufficiently investigated. The relevance of this issue is increasing with the development of active-adaptive networks and the introduction of wind power plants [3, 4].

The theoretical and practical relevance of the problem of higher harmonics in electrical networks is confirmed by a number of publications, both by foreign [5, 6] and domestic specialists [7, 8].

Significant losses in power supply systems associated with low quality electrical energy require additional research into the nature of higher harmonics at industrial enterprises [9, 10]. The results of research into the nature of higher harmonics in power inverters and means of combating them are effectively implemented [11, 12]. Extensive theoretical and practical experience in the quality of energy resources is reflected in normative documents taking into account the European education for the electric power industry of our country.

Modern trends in the development of electrical networks, namely, the introduction of active-adaptive networks, introduce new aspects regarding the quality of electrical energy [13, 14]. This requires constant control of power quality parameters, and in particular the levels of higher harmonics, in real time [15,16]. The study of the nature of individual harmonics is of significant practical importance. This is confirmed by the study of, for example, third (saturation of the magnetic circuit) and toothed harmonics, which appear as a result of the unevenness of the air gap of rotating electric machines [17,18]. Therefore, the study of groove harmonics is relevant.

The purpose of the study is to obtain scientific results regarding the nature of groove harmonics of rotating electric machines and to establish the characteristics of their distribution in distribution electrical networks. To achieve the purpose, the following objectives were set:

- to develop a methodology for calculating currents and electromotive force of the groove frequency of rotary electric machines for active-adaptive networks;
- determine the dependences of the levels of groove harmonics of the electrical network.

2. Results

Higher harmonics of distribution electrical networks have a constructive or technological nature. Each harmonic component has one or more sources and a defined propagation space. The amplitude value of the higher harmonic and its flow paths are determined by the interaction of the inductive and capacitive elements of the electrical network. The most unpleasant case is the case of resonance of higher current or voltage harmonics in electrical networks and large enterprises. The manifestation in time determines the random or systematic nature of higher harmonics [19, 20].

In the process of operation, electric rotary machines generate groove harmonics in the electrical network [21, 22]. The appearance of these harmonics is related to the magnetomotive force of the rotor winding. Their frequency can be determined by the expression:

$$\omega_n = \omega_1 \cdot \left[\frac{z_n}{p} \cdot (1 - S) \pm 1\right], \tag{1}$$

where ω_1 is the cyclic frequency; z_n is the number of grooves on the rotor; p is the number of pairs of poles; S is the slip.

The amplitude value of these harmonics is determined by the design parameters of the electric machine and the network voltage. The significant danger of groove harmonics is caused by the dependence of these frequencies on the network frequency and slippage, which can lead to resonance phenomena [23, 24].

Determining the levels of higher harmonics by experimental removal of curves taking into account electromagnetic asymmetry on real electric machines is associated with a large amount of labor, due to the need to manufacture special calibration stands [25, 26].

Finding by calculation the values of higher harmonics corresponding to the maximum permissible asymmetry of the electric machine allows to avoid working with bulky calibration stands. In this case, only verification tests of several electric motors are required [27, 28].

The method of calculating the energy level of higher harmonics in the form of the sum of the squares of the electromotive force of the groove harmonics, taken when each of the three phases of the stator winding is turned off in sequence, is based on the determination of the dependence of magnetic losses from the groove harmonics of the magnetic field in the air gap on the degree of electromagnetic asymmetry [29, 30].

The energy level of the slot frequency induction harmonics characterizes the magnetic losses in steel from the slot order magnetic field. Specific magnetic losses in steel are determined by the expression:

$$P_{mg} = \varepsilon_g \cdot \frac{f}{50} \cdot B^2 + \sigma \cdot \left(\frac{f}{50}^2\right) \cdot B^2, \tag{2}$$

where P_{mg} is the specific magnetic losses in steel; ε_g is the specific losses from hysteresis at $f = 50$ Hz and $V = 1$ T; σ is the specific losses from eddy currents at $f = 50$ Hz and $V = 1$ T; B is the magnetic induction; f is the frequency of magnetic induction.

The specific magnetic losses in steel from the groove harmonics of induction are determined by the expression:

$$P_{mg} = \varepsilon_g \cdot \frac{f}{50} \cdot \frac{1}{2\pi \cdot T_z} \cdot \int_0^{2\pi}\int_0^{T_z} B_n^2(\varphi, t) d\varphi \cdot dt + \sigma \cdot \left(\frac{f_n}{50}\right)^2 \cdot \frac{1}{2\pi \cdot T_n} \cdot \int_0^{2\pi}\int_0^{T_n} B_n^2(\varphi, t) d\varphi \cdot dt, \tag{3}$$

where $f_n = \frac{\omega_n}{2\pi}$ is the electrical frequency of the groove harmonic of induction; $T_z = \frac{2\pi}{\omega_z}$ is the the period of the groove harmonic of the induction; $K_n = \varepsilon_g \cdot \frac{f_z}{50} + \sigma \cdot (\frac{f_n}{50})^2$ is the power loss factor; $B_n(\varphi, t)$ is the spatio-temporal distribution of magnetic field induction in a gap with electromagnetic asymmetry; ω_n is the angular frequency of the groove harmonic of induction (upper and lower).

Will find the specific magnetic losses from the upper slot harmonic of the induction with frequency $\omega_{up} = \omega_1 \cdot [\frac{z_n}{p} \cdot (1 - S) + 1]$ in the three-phase mode of operation, substituting the expression for the spatio-temporal distribution of the slot frequency induction for the three-phase mode:

$$P_{mgup} = K_n \cdot \frac{1}{2\pi \cdot T_n} \cdot \int_0^{2\pi}\int_0^{T_n} B_{up}^2(\varphi, t) d\varphi \cdot dt, \tag{4}$$

Integrating within the range from 0 to 2π and taking into account that for an even whole number, all components containing factors of the form $\sin k \cdot \pi \cdot (Z_1 \pm n)$, where k and n are the integers, obtain the final expression for specific magnetic losses from the upper slot frequency of induction, taking into account the spatial distribution of conductivity air gap with asymmetry and the obtained expressions for the coefficients of the series $\lambda_{\alpha 0}$ and λ_n :

$$P_{mgup} = \frac{1}{16} \cdot K_n \cdot (\lambda_0 \cdot \lambda_{j1} \cdot F_1)^2 \cdot \left(\frac{1}{2} \cdot \lambda_{\alpha 0}^2 + \frac{1}{4} \cdot \lambda_{\alpha 0}^2 + \lambda_{n1}^2 + \frac{1}{2} \cdot \lambda_{i1}^2 \cdot \lambda_{n1}^2\right), \tag{5}$$

In this expression $\frac{1}{2} \cdot \lambda_{\alpha 0}^2 + \lambda_{n1}^2 = K_{\alpha 1}$ there is a coefficient of losses due to magnetic asymmetry, taking into account only the first term of the series λ_n . According to mathematical transformations:

$$K_{\alpha 1} = \frac{8 - 2 \cdot a_m^2 - 8 \cdot \sqrt{1 - a_m^2}}{a_m^2 \cdot (1 - a_m^2)}, \tag{6}$$

where a_m is the coefficient of relative electromagnetic asymmetry.

Carrying out similar transformations taking into account the first two and three terms of the series, it is possible to obtain the corresponding coefficients $K_{\alpha 2}$ and $K_{\alpha 3}$, which refine the calculation:

$$K_{\alpha 2} = \frac{1}{2} \cdot \lambda_{\alpha 0}^2 + \lambda_{n1}^2 + \lambda_{n2}^2; \tag{7}$$

$$K_{\alpha 3} = \frac{1}{2} \cdot \lambda_{\alpha 0}^2 + \lambda_{n1}^2 + \lambda_{n2}^2 + \lambda_{n3}^2. \tag{8}$$

In the general case, taking into account all terms of the Fourier series, the expression for the specific magnetic losses from the upper slot frequency of induction will have the form:

$$P_{mgup} = \frac{1}{16} \cdot K_{\alpha n} \cdot (\lambda_0 \cdot \lambda_{j1} \cdot F_1)^2 \cdot \left(1 + \frac{1}{2} \cdot \lambda_{i1}^2\right) \cdot K_{\alpha n}, \tag{9}$$

where $K_{\alpha n}$ is the electromagnetic asymmetry coefficient taking into account the terms of the Fourier series λ_n.

$$K_{\alpha n} = \frac{1}{2} \cdot \lambda_{\alpha 0}^2 + \sum_{n=1}^{\infty} \lambda_n^2 = \frac{4}{1 - a_m^2} \cdot \left[\frac{1}{2} + \sum_{n=1}^{\infty} \left(\frac{1 - \sqrt{1 - a_m^2}}{a_m}\right)^{2n}\right]. \tag{10}$$

Since at any values $0 < a_m < 1$ the values of the function $q = \left(\frac{1-\sqrt{1-a_m^2}}{a_m}\right)^2$ are also in the range from 0 to 1 (figure 1), the sum will have a finite value and the expression for $K_{\alpha n}$ in its final form will have the form:

$$K_{\alpha n} = \frac{4}{1 - a_m^2} \cdot \left[\frac{1}{2} + \frac{1 - \sqrt{1 - a_m^2}}{a_m^2 - (1 - \sqrt{1 - a_m^2})^2}\right]. \tag{11}$$

Thus, the specific magnetic losses from the upper slot harmonic of the induction depend on the value of the relative electromagnetic asymmetry. The nature of this dependence is completely determined by the nature of the graph.

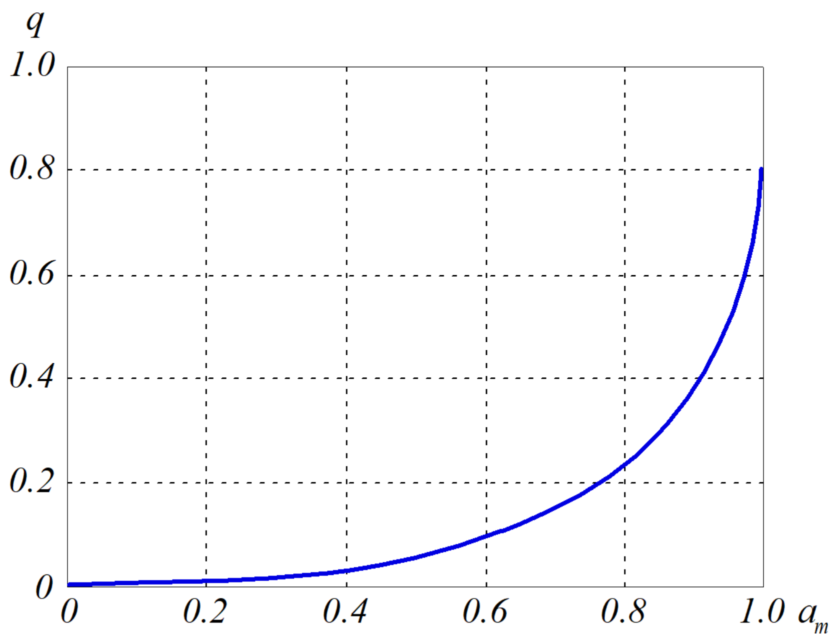

Figure 1. Range of function values $q = \left(\frac{1-\sqrt{1-a_m^2}}{a_m}\right)^2$.

When determining the losses by the coefficient $K_{\alpha n}$, taking into account only the first two members of the harmonic series λ_n the relative error of the calculation γ_n with an electromagnetic asymmetry of up to 50% does not exceed 2%, and then it begins to grow monotonically, and in the region of large asymmetry ($a_m = 80 + 90\%$) is 10 + 25% (figure 2).

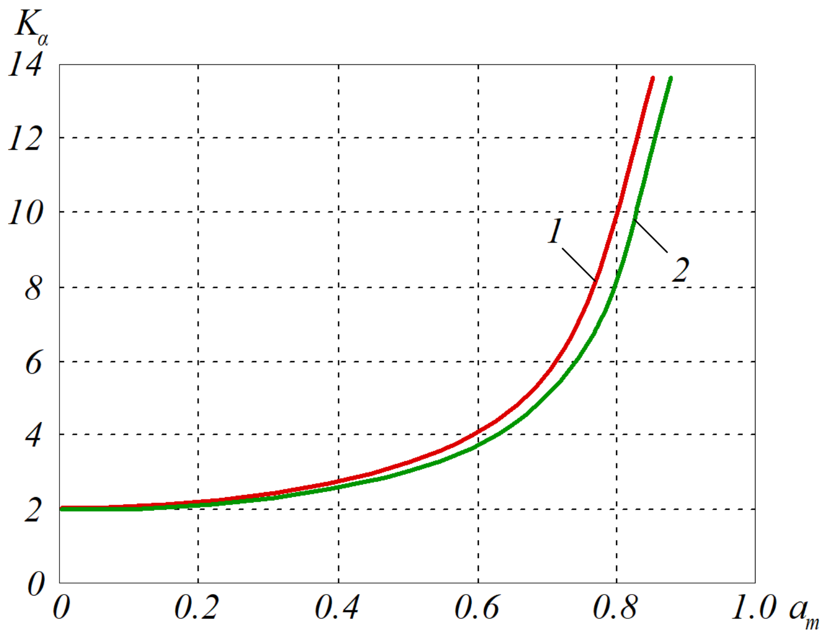

Figure 2. Dependence of magnetic loss increase coefficients on electromagnetic asymmetry: 1 – dependence $K_{\alpha n} = f(a_m)$;, 2 – dependence $K_{\alpha 1} = f(a_m)$.

Calculation of the third term of the harmonic series λ_n significantly increases the accuracy of the calculation. The error $\gamma_{\alpha 2}$ in determining losses by the coefficient $K_{\alpha 2}$ does not exceed 2% with asymmetry up to 80% and increases to 8 + 10% with an increase in electromagnetic asymmetry up to 90% (figure 3).

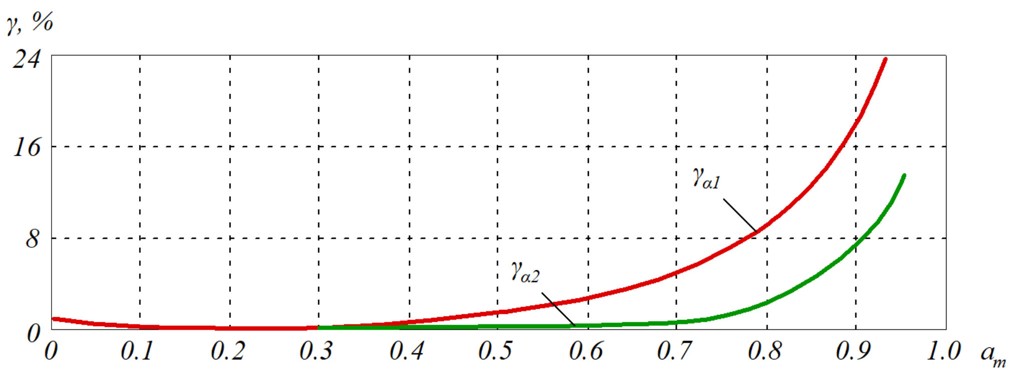

Figure 3. Change in the relative errors of the calculation of magnetic losses from groove harmonics of the field by coefficients.

Let us determine the specific magnetic losses in steel from the first groove harmonic of induction when the electric motor is operating in the phase-disconnected mode, substituting the expression for the spatio-temporal distribution of the groove frequency induction in (4) for the single-phase mode, taking into account the full distribution λ_n:

$$P'_{mgup} = K_n \cdot \frac{1}{2\pi \cdot T_n} \cdot \int_0^{2\pi} \int_0^{T_n} B_{fup}^2(\varphi, t) d\varphi \cdot dt. \tag{12}$$

Opening the brackets and integrating in a similar way, obtain the final expression for specific magnetic losses in steel from the first (upper) slot harmonic of induction in the form:

$$P'_{mgup} = \frac{1}{32} \cdot K_n \cdot (\lambda_0 \cdot \lambda_{j1} \cdot F_f)^2 \cdot \left(1 + \frac{1}{2} \cdot \lambda_{i1}^2\right) \cdot K_{\alpha n}, \tag{13}$$

where F_f is the magnetizing force when working on two phases; $K_{\alpha n}$ is the coefficient of electromagnetic asymmetry.

Thus, the nature of the dependence of the specific magnetic losses in steel on the groove harmonics of induction when the machine is operating in the mode with a disconnected phase is similar to the nature of this dependence for the three-phase mode and is determined by the type of function $K_{\alpha n} = f(a_m)$.

The quantitative ratio of losses during the operation of the electric motor in three-phase mode and in the mode with a disconnected phase can be estimated through the coefficient of proportionality of losses:

$$P'_{mgup} = K_f \cdot P_{mgup}, \tag{14}$$

where K_f is the proportionality factor $K_f = \frac{P'_{mgup}}{P_{mgup}}$; I_{vf} is the phase current in the phase-disconnected mode; I_{tf} is the phase current in three-phase mode; W is the the number of turns in a phase; k_o is the winding ratio.

Assuming that the phase resistance complexes at the fundamental frequency are approximately equal and the linear voltage to the root of three is greater than the phase voltage, obtain:

$$K_f = \frac{2}{3} \cdot \left(\frac{\sqrt{3}}{2}\right)^2 = \frac{1}{2}. \tag{15}$$

In a similar way, the specific magnetic losses from the lower groove harmonic of the induction, which varies in time with the frequency ω_n , can be calculated for both modes of operation of the machine. The total specific magnetic losses from the groove fields of the first order will be equal to the doubled value of P_{mgup} and P'_{mgup}.

Electromagnetic asymmetry significantly affects the nature of the distribution of the magnetic field in the air gap of the electric machine. In the presence of non-symmetry, the amplitudes of groove harmonics of magnetic induction increase.

The increase in the amplitude of the magnetic induction of higher harmonics of the magnetic field causes a sharp increase in magnetic losses from groove harmonics with an increase in electromagnetic asymmetry in accordance with the dependence $K_{\alpha n} = f(a_m)$. A significant increase in additional losses with an increase in electromagnetic asymmetry is also confirmed by a number of experimental studies.

The groove harmonic components of the magnetic field in the air gap induce electromotive force in the stator windings with frequencies ω_n.

In the conductor of each groove of the stator winding, an electromotive force of the groove frequency is induced, which is proportional to the change in induction. Accordingly, the square of the electromotive force will be proportional $B_n^2(\varphi, t)$ and proportional to the pulsation losses in the steel from the groove harmonics of induction P_{mgn} in the elementary volume of the groove zone near the k-th groove. Then the sum of the squares of the electromotive force in the conductors of all the slots of the stator winding will be proportional to the total magnetic losses of the electric machine from the slot harmonics of the field in the gap, and since the level of pulsation losses depends on the degree of electromagnetic asymmetry, the value will, other things being equal, be proportional to the energy level of the slot harmonics and will by some asymmetry function.

The dependence of the magnetic losses of the slot induction field from the similar dependence in the three-phase mode differs by a constant volume factor by summing the squares of the electromotive force of the slot frequency, given in all three phases of the stator winding, when each of them is sequentially disconnected, it is possible to obtain an indirect diagnostic parameter, that is a function of the unevenness of the electromagnetic system, since in the case of the specified summation, all n grooves of the stator winding are taken into account, which is similar to the integration over the stator boring circle. The degree of change of the obtained parameter with increasing electromagnetic asymmetry is determined by the nature of the dependence of pulsating magnetic losses on the asymmetry of the electromagnetic system.

The electromotive force of the groove frequency arising in the coil of the stator winding, which contains W turns, the sides of which lie in the grooves with angular coordinates φ_k and φ_n is defined as the time derivative of the flux linkage:

$$e_{kn}(t) = -\frac{d\psi_n}{dt}, \tag{16}$$

where ψ_n is the magnetic flux and flux coupling of toothed harmonics with turns of the stator winding.

In its general form, this expression can be given by the formula of harmonic oscillation:

$$e_{kn}(t) = E_{kn} \cdot \sin(\omega_{up} \cdot t - Q_{kn}); \tag{17}$$

$$E_{kn} = \sqrt{\left(\sum_{i=1}^{18} E_i \cdot \cos Q_i\right)^2 + \left(\sum_{i=1}^{18} E_i \cdot \sin Q_i\right)^2}; \tag{18}$$

$$\begin{cases} \arctan = \dfrac{\sum_{i=1}^{18} E_i \cdot \sin Q_i}{\sum_{i=1}^{18} E_i \cdot \cos Q_i}, & \text{if } \sum_{i=1}^{18} E_i \cdot \sin Q_i \neq 0; \sum_{i=1}^{18} E_i \cdot \cos Q_i \neq 0; \\ \frac{\pi}{2}, & \text{if } \sum_{i=1}^{18} E_i \cdot \sin Q_i = 0; \sum_{i=1}^{18} E_i \cdot \cos Q_i > 0; \\ \frac{3\pi}{2}, & \text{if } \sum_{i=1}^{18} E_i \cdot \sin Q_i = 0; \sum_{i=1}^{18} E_i \cdot \cos Q_i < 0, \end{cases} \tag{19}$$

where E_i is the amplitudes of harmonic components of the electromotive force coil; Q_i is the initial phases of harmonic components of the electromotive force coil.

The total electromotive force induced in the disconnected phase without parallel branches can be found by summing the electromotive force of the turns that make up the phase winding.

When disconnecting the next phase and determining the electromotive force of the groove harmonic in its winding, the value ψ_f and coordinates of the distribution of turns change.

If the disconnected phase of the stator winding contains N parallel-connected coil groups, then the electromotive force of the groove harmonic phase is equal to:

$$e_f(t) = \frac{1}{N} \cdot \left[e_{r1}(t) + e_{r2}(t) + ... + e_{rn}(t)\right], \tag{20}$$

where $e_{rn}(t)$ is the electromotive force of coil groups, defined as the sum of the electromotive forces of the component turns.

In the case of mixed connection of coil groups in phase, the electromotive force of parallel sections is determined by expression (17) and then summed up with all groups connected in series.

The amplitude of the electromotive force of the groove harmonic of a separate phase of the stator winding can either increase with an increase in electromagnetic asymmetry ψ_α with respect to the distribution of the turns of a given phase, or decrease, while the sum of the squares of the electromotive force of the groove harmonic of all three phases uniquely increases with increasing α, reflecting an increase in pulsation losses at presence of asymmetry, close to quadratic in nature.

Thus, according to the proposed method, the energy level of higher harmonics can be estimated by the sum of the squares of the electromotive force of the groove harmonics, taken when each of the three phases of the stator winding is turned off sequentially when the tested machine is idling. In order to exclude the influence of saturation phenomena on the control result and to reduce current overloads of the electric motor when operating in the mode with a disconnected phase, the measurement must be carried out when the two working phases of the winding are powered with a reduced single-phase voltage.

To refine theoretical calculations near the extreme points of the range of asymmetry values, a technique for presenting the amplitude of groove harmonics of magnetic induction in an air gap with two-way groove through the Carter coefficient, taking into account its dependence on electromagnetic asymmetry, is proposed:

$$B_n = B_m - B_{\alpha v}, \tag{21}$$

where B_n is the amplitude of the groove harmonic of induction; $B_{\alpha v}$ is the average value of induction with electromagnetic symmetry; B_m is the maximum value of induction.

Coefficients determined by the ratio of the groove opening width to the gap size:

$$\gamma_1(\varphi) = \frac{\left[\frac{B_{s1}}{\delta(\varphi)}\right]^2}{5 + \frac{B_{s1}}{\delta(\varphi)}}; \tag{22}$$

$$\gamma_2(\varphi) = \frac{\left[\frac{B_{s2}}{\delta(\varphi)}\right]^2}{5 + \frac{B_{s2}}{\delta(\varphi)}}. \tag{23}$$

Obtain the final expression for the amplitude of the groove harmonic of magnetic induction in an air gap with two-sided groove:

$$B_{\alpha v} = \frac{5 \cdot (t_{z1} \cdot B_{s2}^2 + t_{z2} \cdot B_{s1}^2) \cdot \delta(\varphi) + B_{s1} \cdot B_{s2} \cdot (t_{z1} \cdot B_{s2} + t_{z2} \cdot B_{s1} - B_{s1} \cdot B_{s2})}{\left[t_{z1} \cdot (5 \cdot \delta(\varphi) + B_{s1}) - B_{s1}^2\right] \cdot \left[t_{z2} \cdot (5 \cdot \delta(\varphi) + B_{s1}) - B_{s2}^2\right]}; \tag{24}$$

Using the method of determining the electromotive force, will obtain a general final expression for one phase of the upper groove frequency of the first order in the form of harmonic oscillation:

$$e_f(t) = E \cdot \sqrt{A_t^2 + B_t^2} \cdot \sin\left[\omega_{up} \cdot t + \arctan\left(-\frac{A_f}{B_f}\right)\right]; \tag{25}$$

$$E = E_t = -\frac{3 \cdot \sqrt{2} \cdot \mu_0 \cdot I \cdot l_\delta \cdot D_c \cdot W^2 \cdot k_b \cdot \omega_{up}}{4 \cdot \pi \cdot \delta_0 \cdot N_k \cdot p}; \tag{26}$$

$$A_f = \sum_{N=1}^{N_k} \int_{\varphi_k N_f}^{\varphi_n N_f} [k_\delta(\varphi) - 1] \cdot \sin(Z_2 + p) \cdot \varphi \cdot d\varphi, \tag{27}$$

where D_c is the stator diameter; N_k is the number of turns in the phase.

Accordingly, for the mode of operation of an asynchronous electric motor with a disconnected phase:

$$E = E_f = -\frac{\sqrt{6} \cdot \mu_0 \cdot I \cdot l_\delta \cdot D_c \cdot W^2 \cdot k_b \cdot \omega_{up}}{2 \cdot \pi \cdot \delta_0 \cdot N_k \cdot p}; \tag{28}$$

$$A_f = \sum_{N=1}^{N_k} \int_{\varphi_k N_f}^{\varphi_n N_f} [k_\delta(\varphi) - 1] \cdot \cos(p \cdot \varphi - \psi_f) \cdot \sin Z_2 \cdot \varphi \cdot d\varphi, \tag{29}$$

$$B_f = \sum_{N=1}^{N_k} \int_{\varphi_k N_f}^{\varphi_n N_f} [k_\delta(\varphi) - 1] \cdot \cos(p \cdot \varphi - \psi_f) \cdot \cos Z_2 \cdot \varphi \cdot d\varphi. \tag{30}$$

The dependence of the electromotive force of the groove harmonic of individual phases and the sum of the squares of their amplitudes on the magnitude of the electromagnetic asymmetry was calculated on an electronic computer. The calculation algorithm is built on the basis of the above mathematical apparatus using the given expressions.

As expected, the graphical form of the theoretical dependence of the sum of the squares of the electromotive force of the groove harmonic on the electromagnetic asymmetry, calculated according to the given mathematical model, is similar to the dependence $K_{en} = f(e)$.

The proposed technique allows determining the energy levels of higher harmonics not only taking into account the value of absolute and relative asymmetry, but also taking into account the direction in space of the plane of asymmetry in relation to the distribution of the stator windings.

The initial value for determining the spatial angle of the direction of the plane of asymmetry is obtained from the expression of the electromotive force of the groove harmonic from any disconnected phase of the stator winding, assuming that α, δ_0, E_{nA} are the values obtained by the expressions:

$$E_{nA} = E \cdot \sqrt{A_A^2 + B_A^2}; \tag{31}$$

$$A_A^2 + B_A^2 = \frac{E_{nA}^2}{E^2}, \tag{32}$$

where E is the general constant that does not depend on φ and t; A_A, B_A are the sums of definite integrals.

The algorithm for calculating the dependence of the electromotive force of the groove harmonic on the electromagnetic asymmetry is presented in (figure 4).

By replacing and introducing a new variable and bringing similar terms, will finally get the equation in the canonical form:

$$x^4 + a \cdot x^3 + b \cdot x^2 + c \cdot x + d = 0; \tag{33}$$

$$a = \frac{2 \cdot (A \cdot B + C \cdot D)}{A^2 + D^2}; \tag{34}$$

$$b = \frac{2 \cdot A \cdot M + B^2 + C^2 - D^2}{A^2 + D^2}; \tag{35}$$

$$c = \frac{2 \cdot (B \cdot M + C \cdot D)}{A^2 + D^2}; \tag{36}$$

$$d = \frac{M^2 - C^2}{A^2 + D^2}; \tag{37}$$

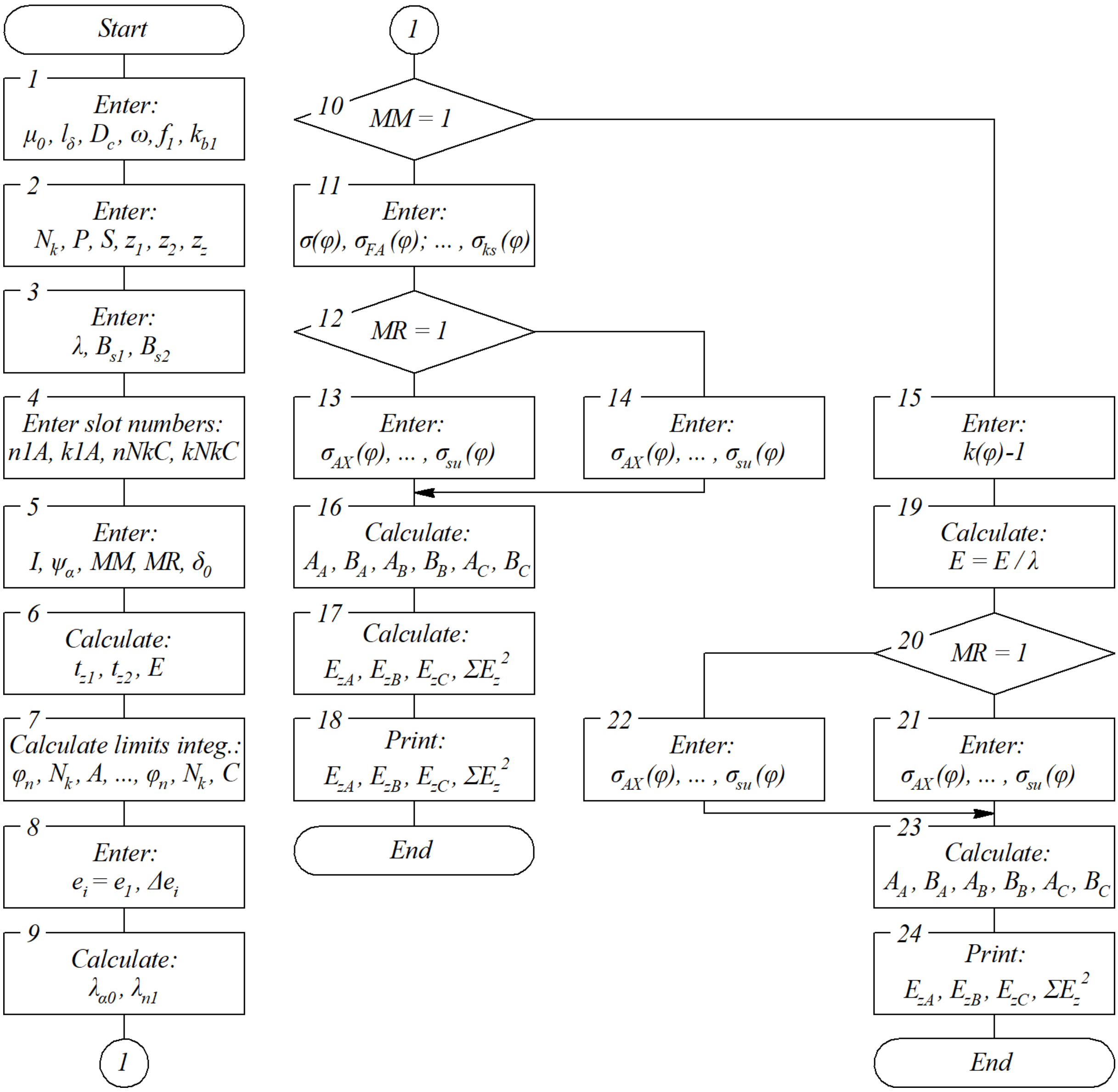

Figure 4. Calculation algorithm.

$$A = \lambda_{n1}^2 \cdot (C_2^2 + C_5^2 - C_3^2 - C_6^2); \tag{38}$$

$$B = \lambda_{\alpha 0} \cdot \lambda_{n1} \cdot (C_1 \cdot C_2 + C_4 \cdot C_5); \tag{39}$$

$$C = \lambda_{\alpha 0} \cdot \lambda_{n1} \cdot (C_1 \cdot C_3 + C_4 \cdot C_6); \tag{40}$$

$$D = 2 \cdot \lambda_{n1}^2 \cdot (C_2 \cdot C_3 + C_5 \cdot C_6); \tag{41}$$

$$C_1 = \sum_{N=1}^{N_k} \int_{\varphi_k N_A}^{\varphi_n N_A} \sigma'_A(\varphi) \cdot \sin Z_2 \cdot \varphi \cdot d\varphi; \tag{42}$$

$$C_2 = \sum_{N=1}^{N_k} \int_{\varphi_k N_A}^{\varphi_n N_A} \sigma'_A(\varphi) \cdot \cos\varphi \cdot \sin Z_2 \cdot \varphi \cdot d\varphi; \tag{43}$$

$$C_3 = \sum_{N=1}^{N_k} \int_{\varphi_k N_A}^{\varphi_n N_A} \sigma'_A(\varphi) \cdot \sin\varphi \cdot \sin Z_2 \cdot \varphi \cdot d\varphi; \quad (44)$$

$$C_4 = \sum_{N=1}^{N_k} \int_{\varphi_k N_A}^{\varphi_n N_A} \sigma'_A(\varphi) \cdot \cos Z_2 \cdot \varphi \cdot d\varphi; \quad (45)$$

$$C_5 = \sum_{N=1}^{N_k} \int_{\varphi_k N_A}^{\varphi_n N_A} \sigma'_A(\varphi) \cdot \cos\varphi \cdot \cos Z_2 \cdot \varphi \cdot d\varphi; \quad (46)$$

$$C_6 = \sum_{N=1}^{N_k} \int_{\varphi_k N_A}^{\varphi_n N_A} \sigma'_A(\varphi) \cdot \cos Z_2 \cdot \sin\varphi \cdot \varphi \cdot d\varphi. \quad (47)$$

Thus, the desired angle ψ_α is determined through the roots of the reduced equations:

$$\psi_\alpha = \arccos x. \quad (48)$$

Of the four roots of expression (33), two are imaginary, and the two real roots give, respectively, a positive and a negative angle ψ_α calculated from the stator boring from the axis that coincides with the axis of the phase A winding.

The developed technique makes it possible to determine the levels of groove harmonic components in the phase windings of electric machines. These harmonics, depending on the connection scheme of the asynchronous motor windings (star, delta), the scheme and the load of the electrical network, spread over the electrical network, creating current harmonics or voltage harmonics. When analyzing asymmetric and non-sinusoidal modes at individual frequencies, various harmonic components arise, which leads to the emergence of specific current and voltage harmonics. All these phenomena must be taken into account when analyzing the modes of distribution networks.

The current level of development of electronic computers and their software allows to form mathematical models of the electrical network at the groove frequency in asymmetric modes, considering all its elements as three-phase. At the same time, equations in phase coordinates serve as mathematical models of both the network as a whole and its individual elements – equations containing mode parameters (voltages, currents, phase powers) as sought and set values.

Equations in phase coordinates refer to the electrical network, the elements of which are three-phase longitudinal and transverse branches. Longitudinal branches are contained in the schemes of substitution of sections of power transmission lines, three-phase windings of generators and transformers, transverse branches correspond to schemes of substitution of load nodes, transverse conductances of sections of overhead lines, branches of magnetization of transformers.

Each branch of the three-phase network is characterized by a matrix of own and mutual resistances of the phases:

$$[Z]_{ij}^F = \begin{bmatrix} Z_{aa} & Z_{ab} & Z_{ac} \\ Z_{ba} & Z_{bb} & Z_{bc} \\ Z_{ca} & Z_{cb} & Z_{cc} \end{bmatrix}_{ij}, \quad (49)$$

where the diagonal elements Z_{aa}, Z_{bb}, Z_{cc} reflect the active and inductive resistances of the respective phases, and non-diagonal resistances – the mutual induction between phases, and mode parameters – currents, voltages, electromotive forces of the phases.

$$[I]_{ij}^{F} = \begin{bmatrix} I_a \\ I_b \\ I_c \end{bmatrix}_{ij}; \tag{50}$$

$$[U]_{ij}^{F} = \begin{bmatrix} U_a \\ U_b \\ U_c \end{bmatrix}_{ij}; \tag{51}$$

$$[E]_{di}^{F} = \begin{bmatrix} E_a \\ E_b \\ E_c \end{bmatrix}_{ij}. \tag{52}$$

In asymmetric emergency modes, loads are characterized by conductance matrices in the node to the ground:

$$[Y_H]^F = [Z_H^F]^{-1}. \tag{53}$$

In non-symmetric operating modes (non-linear model), the load conductivity matrices (53) are kept unchanged only at the step of the iteration process and are adjusted during the iterations in such a way that the total consumed power of the three phases becomes equal to the set power at the node.

The component equations of the elements of a three-phase network in phase values have the form:

- for longitudinal branches:

$$[Z]_{ij}^{F} \cdot [I]_{ij}^{F} = \left([U]_i^F - [U]_j^F\right); \tag{54}$$

- for transverse branches:

$$[Z]_{Hi}^{F} \cdot [I]_{Hij}^{F} = [U]_i^F; \tag{55}$$

- for branches with a source of electromotive force:

$$[Z]_{di}^{F} \cdot [I]_{di}^{F} = \left([U]_{di}^F - [E]_{di}^F\right). \tag{56}$$

These equations are a generalization of Ohm's law for a three-phase branch and differ from similar equations of elements of a single-phase circuit only in that resistances, currents, electromotive force and voltages of three-phase elements are not characterized by numbers, but by corresponding matrices.

Matrices of both longitudinal $[Z]_{ij}$, and transverse $[Z]_{i0}$ elements can be asymmetrical, symmetrical or, in a separate case (a group of single-phase elements), diagonal. All types of longitudinal and transverse asymmetry (non-transposed overhead lines, network elements operating with an incomplete number of phases, asymmetric loads, etc.) are reflected in the parameter matrices $[Z]$ of the corresponding elements.

A three-phase network can be matched by a graph, the branches of which correspond to three-phase branches, and the nodes to three-phase nodes. Then, for three-phase circuits and three-phase nodes, Kirchhoff's laws can be represented in the form:

$$\sum_{i=1}^{N}[I]_{ij}^{F} = 0; \sum_{i=1}^{N_k}[\Delta U]_{ij}^{F} = 0. \tag{57}$$

where $[I]_{ij}$ is the the currents in the branches adjacent to the three-phase node; $[U]_{ij}$ is the voltage drop on the three-phase branches forming a closed circuit in the three-phase network.

If for all independent three-phase nodes of the electrical networidraw up the current balance equation, solve the component equations of the three-phase branches adjacent to each of the nodes with respect to the currents and substitute them into the first of the equations, then for a network containing n independent three-phase nodes, get the system of equations of the electrical network in the asymmetric stationary mode in phase coordinates:

$$\begin{bmatrix} Y_{11} & Y_{12} & ... & Y_{1n} \\ Y_{21} & Y_{22} & ... & Y_{2n} \\ ... & ... & ... & ... \\ Y_{n1} & Y_{n2} & ... & Y_{nn} \end{bmatrix}^F \cdot \begin{bmatrix} U_1 \\ U_2 \\ ... \\ U_n \end{bmatrix}^F = \begin{bmatrix} J_1 \\ J_2 \\ ... \\ J_n \end{bmatrix}^F . \tag{58}$$

The elements of this system of equations are the 3×3 matrices of the own $[Y_{ii}]$ and mutual $[Y_{ij}]$ conductances of three-phase nodes, the vectors of phase voltages in the nodes of the three-phase network $[U_i]$ and set currents $[J_i] = [Y_i] \cdot [E_i]$ in the nodes of the connection of generating elements.

All asymmetric emergency damage in the electrical network (disconnection of phases, short circuits of individual phases to each other and to the ground, etc.) can be displayed quite simply when forming nodal equations, taking into account the corresponding commutations in nodes and branches of a three-phase network. Moreover, the presence of several asymmetric damages does not lead to any complications in the algorithms for forming and solving nodal equations compared to the case of local damages. Therefore, mathematical models based on equations in phase coordinates are more flexible and universal, applicable for the analysis of non-symmetric modes of operation with both simple and complex asymmetry.

In the linear model of the network (when applying loads with constant phase resistances Z_n = const), the phase voltages in the nodes of the network in the asymmetric mode under consideration are determined by a one-time solution of the equations, in the non-linear model (with the specified powers consumed and generated in the network nodes) the phase voltages are refined during of the iterative process until the sum of the powers of the three phases in each node of the network becomes equal to the given value. It was established that the levels of groove harmonics are determined by the structure and modes of the electrical network, the geometry of the groove zones of the air gap of the electric machine, and its magnetic properties. Theoretical propositions have been confirmed by experimental studies.

3. Conclusions

A method of calculating currents and electromotive force of the groove frequency of rotary electric machines for active-adaptive networks has been developed. Calculations are based on the analysis of the electromagnetic field of the electric machine and methods of calculating non-symmetrical and non-sinusoidal modes of distribution electric networks (phase coordinates method). It was established that the levels of groove harmonics are determined by the structure and modes of the electrical network, the geometry of the groove zones of the air gap of the electric machine, and its magnetic properties.

Acknowledgments

The article was prepared as part of the support of the grant of young scientists of Ukraine "Development of scientific bases for improving energy efficiency and improving the quality of electricity in electricity networks" (State Registration Number 0121U109440).

ORCID iDs
I V Khomenko https://orcid.org/0000-0002-5141-5391
V P Nerubatskyi https://orcid.org/0000-0002-4309-601X
O A Plakhtii https://orcid.org/0000-0002-1535-8991
D A Hordiienko https://orcid.org/0000-0002-0347-5656
D A Shelest https://orcid.org/0000-0001-6095-658X

References
[1] Gundebommu S L, Hunko I, Rubanenko O and Kuchanskyy V 2020 Assessment of the Power Quality in Electric Networks with Wind Power Plants *2020 IEEE 7th International Conference on Energy Smart Systems (ESS)* pp 190–194 URL https://doi.org/10.1109/ESS50319.2020.9160231
[2] Nerubatskyi V, Plakhtii O and Hordiienko D 2021 Control and Accounting of Parameters of Electricity Consumption in Distribution Networks *2021 XXXI International Scientific Symposium Metrology and Metrology Assurance (MMA)* pp 1–4 URL https://doi.org/10.1109/MMA52675.2021.9610907
[3] Lin C, Han G, Du J, Xu T and Peng Y 2021 *IEEE Transactions on Intelligent Transportation Systems* **22** 3697–3706 URL https://doi.org/10.1109/TITS.2020.3028990
[4] Samadi A and Chabanloo R M 2019 Adaptive coordination of overcurrent relays in active distribution networks utilizing a multi-objective optimization approach *2020 14th International Conference on Protection and Automation of Power Systems (IPAPS)* pp 20–25 URL https://doi.org/10.1109/IPAPS49326.2019.9069388
[5] Huang T, Tan L, Wang R, Li C, Li H and Huang X 2020 Research on Suppression of Higher Harmonics in Wireless Power Transmission System *2020 IEEE PELS Workshop on Emerging Technologies: Wireless Power Transfer (WoW)* pp 228–232 URL https://doi.org/10.1109/WoW47795.2020.9291304
[6] Babu M, Roy P and Banerjee R 2020 Harmonic Analysis for Power Loss Minimization in Radial Distribution System *2020 11th International Conference on Computing, Communication and Networking Technologies (ICCCNT)* pp 1–5 URL https://doi.org/10.1109/ICCCNT49239.2020.9225526
[7] Syvokobylenko V F and Lysenko V A 2021 Use of higher harmonics in currents and voltages for phase-to-ground fault protection in medium voltage networks *2021 IEEE 2nd KhPI Week on Advanced Technology (KhPIWeek)* pp 172–176 URL https://doi.org/10.1109/KhPIWeek53812.2021.9569967
[8] Plakhtii O, Nerubatskyi V, Scherbak Y, Mashura A and Khomenko I 2020 Energy efficiency criterion of Power Active Filter in a three-phase network *2020 IEEE KhPI Week on Advanced Technology (KhPIWeek)* p 165–170 URL https://doi.org/10.1109/KhPIWeek51551.2020.9250073
[9] Bebikhov Y V, Egorov A N and Semenov A S 2020 How Higher Harmonics Affect the Electrical Facilities in Mining Power Systems *2020 International Conference on Industrial Engineering, Applications and Manufacturing (ICIEAM)* pp 1–7 URL https://doi.org/10.1109/ICIEAM48468.2020.9111965
[10] Kotsur M I, Bezverkhnia Y S, Yarymbash D S and Kotsur I M 2022 *Electrical Engineering and Power Engineering* (2) 18–29 URL https://doi.org/10.15588/1607-6761-2022-2-2
[11] Dalai S K, Sahu R and Tripathy C S 2020 Harmonic Mitigation in Single-Phase Grid Connected Photovoltaic System Using SPWM Inverter *2020 International Conference on Computational Intelligence for Smart Power System and Sustainable Energy (CISPSSE)* p 1–6 URL https://doi.org/10.1109/CISPSSE49931.2020.9212280
[12] Das A, Anand S and Sahoo S R 2020 Availability Based Load Harmonic Compensation Using PV Inverter *2020 IEEE International Conference on Power Electronics, Drives and Energy Systems (PEDES)* p 1–6 URL https://doi.org/10.1109/PEDES49360.2020.9379672
[13] Xu Q, Ma G, Ding K and Xu B 2020 *IEEE Access* **8** 174489–174494 URL https://doi.org/10.1109/ACCESS.2020.3025377
[14] Li P, Zhang C, Wu Z, Xu Y, Hu M and Dong Z 2020 *IEEE Transactions on Smart Grid* **11**(3) 2245–2256 URL https://doi.org/10.1109/TSG.2019.2950120
[15] Gujar N S, Trivedi N, Gupta V and Sharma S 2018 Development of embedded system for monitoring of real time harmonics *2018 3rd IEEE International Conference on Recent Trends in Electronics, Information & Communication Technology (RTEICT)* p 222–227 URL https://doi.org/10.1109/RTEICT42901.2018.9012413
[16] Yaghoobi J, Zare F and Rathnayake H 2021 *IEEE Journal of Emerging and Selected Topics in Power Electronics* **9**(3) 2868–2880 URL https://doi.org/10.1109/JESTPE.2020.3028312
[17] Al-Rawashdeh A Y, Dalabeeh A, Al-Zeyod A, Samarah A, Qaryouti G and Albarbarawi O 2020 *Bulletin of Electrical Engineering and Informatics* **9**(4) 1677–1684 URL https://doi.org/10.11591/eei.v9i4.1565
[18] Cheng M, Zhu X, Wang Y, Wang R and Wang W 2020 *IEEE Transactions on Energy Conversion* **35**(1) 279–291 URL https://doi.org/10.1109/TEC.2019.2948974

[19] Hu Y, Xu J, Qian H, Bian S and Xie S 2020 Robustness and Harmonics Suppression of Grid-Connected Inverters with Different Grid Voltage Feedforward Compensations in Weak Grid *2020 IEEE 29th International Symposium on Industrial Electronics (ISIE)* p 779–784 URL `https://doi.org/10.1109/ISIE45063.2020.9152568`

[20] Nerubatskyi V, Plakhtii O and Hordiienko D 2022 Efficiency Analysis of DC-DC Converter with Pulse-Width and Pulse-Frequency Modulation *2022 IEEE 41st International Conference on Electronics and Nanotechnology (ELNANO)* p 571–575 URL `https://doi.org/10.1109/ELNANO54667.2022.9926762`

[21] Vadamalu R S and Beidl C 2021 *IEEE/ASME Transactions on Mechatronics* **26**(1) 381–392 URL `https://doi.org/10.1109/TMECH.2020.3022736`

[22] Gonzalez-Abreu A D, Osornio-Rios R A, Jaen-Cuellar A Y, Delgado-Prieto M, Antonino-Daviu J A and Karlis A 2022 *Energies* **15**(5) 1909 ISSN 1996-1073 URL `https://doi.org/10.3390/en15051909`

[23] Joseph S, Pandey S, Sarkar S and Joseph J 2021 *Nanophotonics* **10**(17) 4175–4207 URL `https://doi.org/10.1515/nanoph-2021-0387`

[24] Asci C, Sadeqi A, Wang W, Rezaei Nejad H and Sonkusale S 2020 *Scientific Reports* **10**(1) 1050 ISSN 2045-2322 URL `https://doi.org/10.1038/s41598-020-57773-6`

[25] Bykhovsky D 2022 *Energies* **15**(2) 653 URL `https://doi.org/10.3390/en15020653`

[26] Evestedt F, Pérez-Loya J J, Abrahamsson C J D and Lundin U 2021 *Electrical Engineering* **103**(1) 195–203 ISSN 1432-0487 URL `https://doi.org/10.1007/s00202-020-01069-5`

[27] Koteleva N I, Korolev N A and Zhukovskiy Y L 2021 *Energies* **14**(20) 6677 URL `https://doi.org/10.3390/en14206677`

[28] Jiang M, Tian J, Goh H H, Yi J, Li S, Zhang D and Wu T 2022 *Energy Reports* **8** 332–342 ISSN 2352-4847 The 2022 International Conference on Energy Storage Technology and Power Systems

[29] Ahmed M, Nahid-Al-Masood and Aziz T 2021 *Energy Reports* **7** 6273–6291 ISSN 2352-4847 URL `https://doi.org/10.1016/j.egyr.2021.09.072`

[30] Li J, Fang H, Liao C and Du J 2020 *IEEE Access* **8** 119071–119081 URL `https://doi.org/10.1109/ACCESS.2020.3001031`